Journal of Luminescence 132 (2012) 2769–2774

Contents lists available at SciVerse ScienceDirect

Journal of Luminescence

journal homepage: www.elsevier.com/locate/jlumin

Multi-spectroscopic techniques to evaluate the toxicity of alloyed CdSeS quantum dots

Hong-Ju Zhan [a,b], Pei-Jiang Zhou [a,*], Ling Ding [a,c], Zhen-Yu He [a,d], Rong Ma [a]

[a] School of Resource and Environmental Science, Hubei Biomass-Resource Chemistry and Environmental Biotechnology Key Laboratory, Wuhan University, Wuhan 430079, China
[b] Jingchu University of Technology, Jingmen 448000, China
[c] College of Chemical Engineering and Technology, Wuhan University of Science and Technology, Wuhan 430081, China
[d] Wuhan Centers for Disease Prevention and Control, Wuhan 430022, China

ARTICLE INFO

Article history:
Received 11 February 2012
Received in revised form
2 April 2012
Accepted 16 April 2012
Available online 22 May 2012

Keywords:
Alloyed quantum dots
Microwave synthesis
Static quenching
Bovine serum albumin

ABSTRACT

Alloyed CdSeS quantum dots (QDs) were successfully synthesized in aqueous phase using microwave irradiation. UV–vis spectroscopy, fluorescence spectroscopy, transmission electron microscopy (TEM) and X-ray diffraction (XRD) techniques proved that the prepared alloyed QDs are composed of a CdSe-rich core and thick CdS shell with homogeneous size distributions. In order to study its biological toxicity, multi-spectroscopic techniques were adopted to investigate their conjugation with BSA. Fluorescence quenching methods indicated the prepared CdSeS QDs strongly quenched the fluorescence of BSA due to the formation of non-fluorescence ground-state complex. UV–vis absorbance spectra, synchronous fluorescence spectra and CD spectra further confirmed the alloyed CdSeS QDs binded with BSA and destroyed their hydrogen bonding networks, which induced the conformation changes of this macromolecule.

1. Introduction

Recently, luminescent semiconductor quantum dots (QDs) have gained a lot of attention for its unique optical and electronic properties such as wide and continuous absorption spectra, narrow and symmetric emission spectra, excellent photostability, high quantum yields and long fluorescence lifetimes [1]. These advantageous features of QDs have endowed them as promising optical probes in biomedicine and biotechnology [2]. Therefore, investigation of QDs' biological toxicity becomes a must before their extensive application [3–7].

In 2006, Hardman reported that the toxicity of QDs depends on physicochemical and environmental factors [8], suggesting that QD size, charge, concentration, coating materials and oxidative, photolytic, and mechanical stability have each been shown to influence QDs toxicity. So it is very complicated to assess the toxicity of QDs through in vitro or in vivo study. Recently, increasing reports have focused on the toxicity study of QDs from the point of molecular biology level.

Bovine serum albumin (BSA) has been one of the most extensively studied proteins because of its medicinal importance, low cost, ready availability, and particularly its structural homology with human serum albumin. BSA molecules are made up of three homologous domains (I–III) which are divided into nine loops (L1–L9) by 17 disulfide bonds. BSA contains two tryptophans, Trp-134 and Trp-212, which possess intrinsic fluorescence, embedded in the first subdomain IB and subdomain IIA, respectively [9,10]. The accessibility of QDs to albumin's fluorophore groups opens the door to understanding the toxicity of QDs on molecular biology level and provides clues to the essential interaction between QDs and BSA [11]. Zhao et al. investigated the biological toxicity of CdTe QDs to BSA via fluorescence spectra, UV–vis absorption spectra and circular dichroism (CD) and showed the addition of CdTe QDs changed the conformation of BSA [12]. Ding et al. proved that L-cysteine capped CdSe/CdS QDs quenches the fluorescence of BSA through the formation of ground state complex [13]. Ghali illustrated that static quenching was responsible for BSA fluorescence quenching upon conjugation with small sized CdS QDs (4.4 nm) [14]. There are also other reports on the interaction between BSA and QDs with bare core or core–shell structure. In contrast, little attention has been paid to the alloyed QDs.

In this paper, alloyed CdSeS QDs were synthesized in aqueous phase via microwave irradiation and were characterized using UV–vis spectroscopy, fluorescence spectroscopy, transmission electron microscopy (TEM) and X-ray diffraction (XRD) techniques. And their biological toxicity was assessed through fluorescence quenching method coupling with UV–vis spectroscopy, synchronous fluorescence spectra and CD spectra.

* Corresponding author. Tel.: +86 27 68766930; fax: +86 27 68778893.
E-mail addresses: 2010102050026@whu.edu.cn (H.-J. Zhan), zhoupj@whu.edu.cn (P.-J. Zhou).

0022-2313/$ - see front matter Crown Copyright © 2012 Published by Elsevier B.V. All rights reserved.
http://dx.doi.org/10.1016/j.jlumin.2012.04.031

2. Experiments

2.1. Materials and device

Selenium powder (Se, 99.8%), anhydrous sodium sulfite (Na_2SO_3, 97%), cadmium chloride hemipentahydrate ($CdCl_2 \cdot 2.5H_2O$, 99%) and 3-mercaptopropionic acid (MPA, 99%) were received from Sigma Aldrich. Bovine serum albumin (BSA, Fraction V, approximately 99%) and other routine chemicals were received from Shenshi Chem. Ltd. All the chemicals were used as received without any purification and ultrapure water (18.2 M Ω cm^{-1}) was used as solvent in all experiments.

2.2. Synthesis of CdSeS QDs

CdSeS QDs were synthesized using Na_2SeSO_3 as the selenium source through a modified literature method [15]. Firstly, 0.30 mol L^{-1} Na_2SeSO_3 solution was obtained via a simple synthesis described by Hankare et al. with some modifications [16]. Briefly, 2.3670 g selenium powder (0.030 mol), 9.453 g sodium sulfite (0.075 mol) and 80 mL ultrapure water were added into a 250 mL three-neck flask and refluxed at 90 °C for 6 h. After cooling down to room temperature naturally, the obtained light yellow solution was transferred into a 100 ml volumetric flask and brought to volume by ultrapure water, which was used as the stock solution of selenium source. The synthesis of CdSeS QDs was conducted on a microwave digestion/extraction system (Milestone, Italy) equipped with some 100 mL exclusive and Teflon inner vessels. Typically, a precursor solution containing Na_2SeSO_3, $CdCl_2$ and MPA was adjusted to pH 9.0 using 1 mol L^{-1} NaOH solution before microwave irradiation. The optimized molar ratio Cd:MPA:Se used in the synthesis was 8:20:1, and the typical concentration of Cd was 1.25 mmol L^{-1}. Then the 50 mL precursor solution was sealed in the digestion vessel and subjected to microwave irradiation at 130 °C for 30 min. After cooling down to room temperature, the as-prepared solution was purified by addition of twice the volume of isopropanol and then centrifugation at 12,000 rpm for 10 min. The colloidal precipitate was redissolved in 2 mL ultrapure water and subjected to freeze–dry in a freeze drier (Christ Alpha 1-2 LD, Germany) to obtain solid powder samples.

2.3. Characterization of the as-prepared QDs

UV–vis absorption measurements were made on a Shimadzu UV-1601 spectrophotometer in a 1 cm path length quartz cuvette. Fluorescence spectra were obtained on a Hitachi F-4500 spectrophotometer equipped with a 150 W xenon lamp and a 1.00 cm quartz cell. X-ray diffraction (XRD) patterns were recorded using a Bruker-Axs D 8 advanced diffractometer with Cu Kα radiation. Transmission electron microscopy (TEM) was performed on a JEOL model JEM 2100 with an acceleration voltage of 200 kV.

2.4. Spectroscopic studies of QDs–BSA interactions

Fluorescence quenching measurements were performed on an F-4500 spectrophotometer and the temperature was controlled by digital aqueous thermostat (Shanghai, China). The stock solution of BSA was dissolved in PBS buffer solution (0.01 mol L^{-1}, pH · 7.40) and kept in refrigerator. When the QDs were manually titrated into the 1.0×10^{-6} mol L^{-1} BSA solution using a micropipette at different temperatures (286 K, 291 K and 296 K), the fluorescent spectra were recorded in the wavelength range 290–440 nm upon excitation at 280 nm.

Synchronous fluorescence spectra were obtained on the F-4500 spectrophotometer by scanning simultaneously the excitation and emission wavelength at 15 or 60 nm intervals.

UV–vis absorption spectra were collected on the Shimadzu UV-1601 spectrophotometer as 1.0×10^{-5} mol L^{-1} BSA solution was titrated by different amounts of QDs solution.

The CD spectra were recorded on a JASCO-J-810 spectropolarimeter (Tokyo, Japan) using a 0.1 cm cell at 0.2 nm intervals with a scanning rate of 100 nm/min. Each spectrum was the average of three successive scans. For the CD experiment, the concentration of BSA dissolved in 0.1 M PBS solution (pH 7.4) was kept at 5.0×10^{-6} mol L^{-1} and QDs added in the BSA–QDs system were 0.625 and 1.250×10^{-6} mol L^{-1}, respectively. After baseline corrections, CD spectra were recorded in the range 200–250 nm at room temperature.

3. Results and discussion

3.1. Structural characterization

UV–vis absorption and fluorescence spectra excited at 354 nm of the prepared QDs recorded at room temperature are shown in Fig. 1. Both the absorption spectra and fluorescence spectra present the characteristic structure of semiconductor nanocrystals. The inset shows that the prepared QDs possessed bright green fluorescence when excited from a 365 nm UV lamp. The calculated quantum yield (QY) was 23.9% according to the method using Rhodamine 6G in ethanol (PLQY=89%) as a reference [17,18]. It is worth noting that the excitonic absorption energy (2.6 eV) of the CdSeS QDs shows a blue shift relative to the absorption gap of bulk CdSe (1.7 eV) and bulk CdS (2.4 eV), which presents significant quantum size effect. Additionally, one can also observe that the shape of fluorescence spectra is very symmetric and full-width at half maximum is relatively narrow (44 nm), implying that the prepared CdSeS QDs have good monodispersity. This also can be confirmed by transmission electron microscopy as presented in Fig. 2, in which the CdSeS QDs exhibit spherical shapes with homogeneous size distributions and the average diameter was estimated to be 2.1 nm.

The prepared QDs were also characterized by powder X-ray diffraction (XRD) patterns and the result was shown in Fig. 3. The broad peaks of XRD implied that the prepared QDs were very small, which is in agreement with the result of TEM. It is also worth noting that, the diffraction pattern evidently shifted toward higher angle, implying that the crystal structure of the

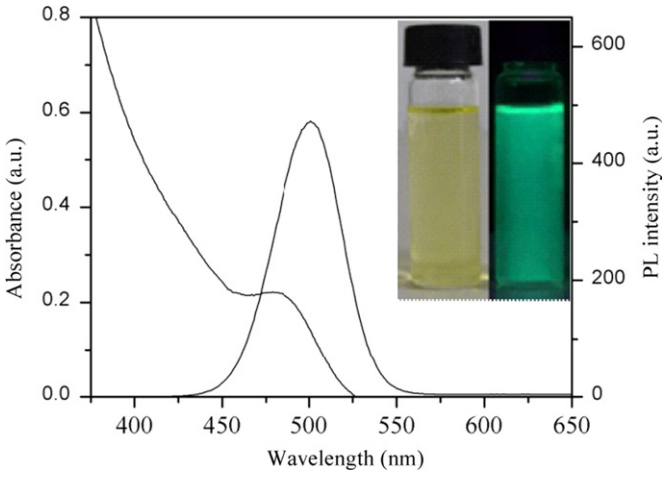

Fig. 1. UV–vis absorption and fluorescence spectra of CdSeS QDs. Inset presents the digital pictures under room light (left) and 365 nm UV (right) radiation.

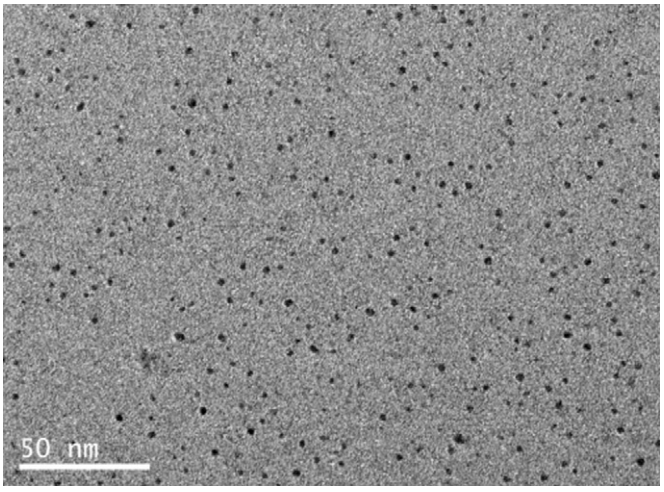

Fig. 2. Transmission electron microscopy (TEM) images of CdSeS QDs. Scale bar is 50 nm.

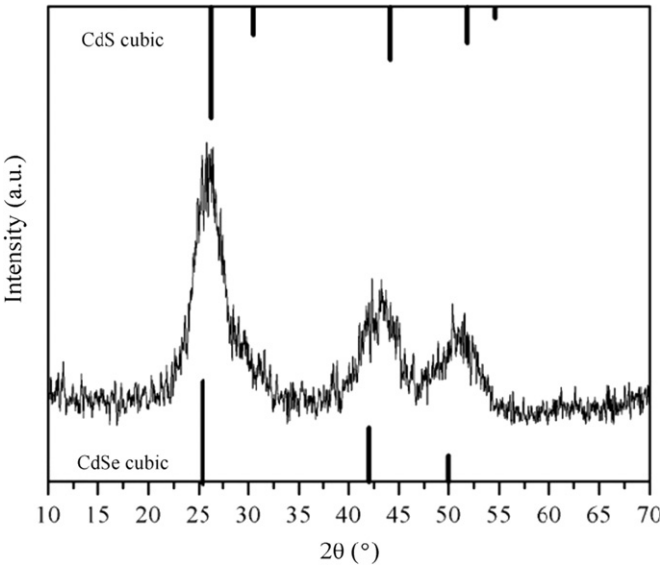

Fig. 3. Powder X-ray diffraction (XRD) patterns of CdSeS QDs. Standard diffraction lines of cubic CdSe and cubic CdS are also shown for comparison.

prepared QDs was quite close to that of bulk cubic CdS, similar to the conclusion illustrated by Qian group [15]. And this conclusion also proved that the prepared QDs are composed of a CdSe-rich core and thick CdS shell, which are called gradient alloyed dots.

3.2. Spectroscopic studies to evaluate the toxicity of CdSeS QDs

In order to evaluate the biological toxicity of the prepared QDs, fluorescence, UV–vis absorption and CD spectra were adopted to investigate the interactions between CdSeS QDs and BSA under simulated physiological conditions.

3.2.1. Fluorescence quenching spectroscopy

The fluorescence quenching of BSA by CdSeS QDs was studied by spectrofluorometry at three temperatures (286 K, 291 K and 296 K). The solution of BSA (1.0×10^{-6} M) was titrated with various concentration of QDs solutions ($0.0–5.12\times10^{-6}$ M) and the fluorescence spectra of BSA were recorded accordingly as shown in Fig. 4. With the addition of QDs solutions, a progressive decrease in the fluorescence intensity of BSA was observed,

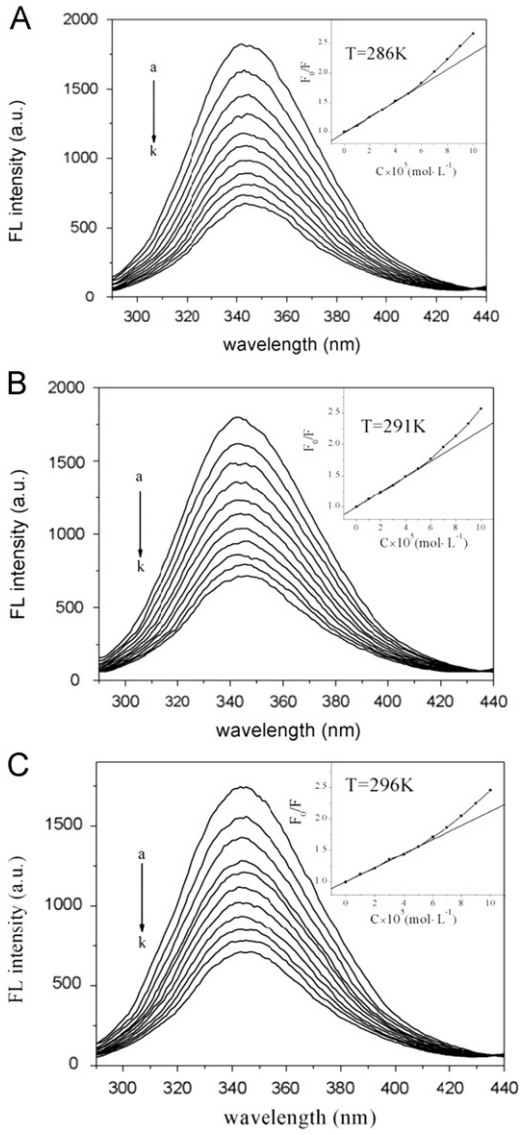

Fig. 4. Fluorescence emission spectra of BSA in the presence of various concentrations of QDs obtained in 0.1 M PBS solution (pH 7.4) and the inset corresponds to Stern–Volmer plots of the quenching of the fluorescence of BSA by QDs at 286 K (A), 291 K (B) and 314 K (C). The concentration of BSA was fixed at 1.0×10^{-6} mol L^{-1}. From (a) to (k), the concentrations of CdSeS QDs were 0, 1.0×10^{-5}, 2.0×10^{-5}, 3.0×10^{-5}, 4.0×10^{-5}, 5.0×10^{-5}, 6.0×10^{-5}, 7.0×10^{-5}, 8.0×10^{-5}, 9.0×10^{-5} and 1.0×10^{-4} mol L^{-1}, successively.

suggesting that interaction between BSA and QDs occured and the interaction induced some changes in the structure of BSA, in agreement with the recent studies in which the tertiary structure of protein (BSA, HSA and IgG) changes was induced by binding of silica-coated CdTe QDs and thiol capped CdTe QDs [19–21].

As is well known, the mechanism of fluorescence quenching can be classified into excited state reactions, energy transfer, collisional quenching (dynamic quenching) and complex formation (static quenching) [22]. In most cases, the last two processes are discussed. In order to clarify the fluorescence quenching mechanism of BSA induced by CdSeS QDs, the Stern–Volmer equation was adoped to process the data [23]:

$$\frac{F_0}{F}=1+K_{sv}[Q]=1+\tau_0K_q[Q]. \quad (1)$$

where F_0 and F are the fluorescence intensities of BSA in the absence and the presence of CdSeS QDs, respectively, [Q] is the

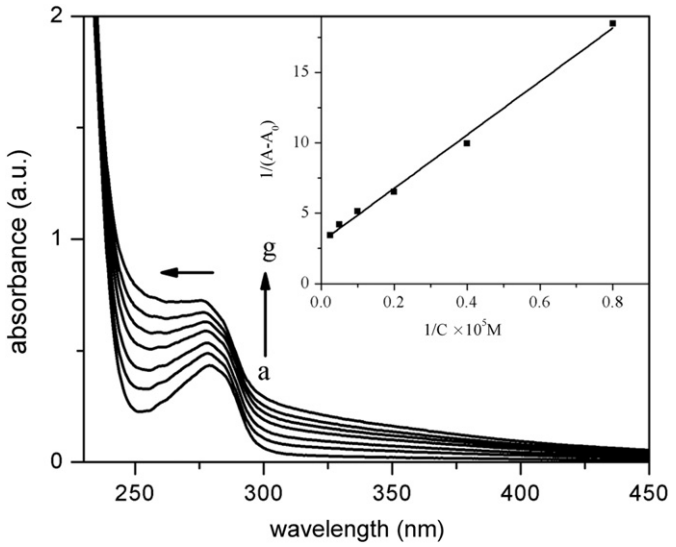

Fig. 5. Absorption spectra of BSA in the presence of different concentrations of CdSeS QDs obtained in 0.1 M PBS solution (pH 7.4). The concentration of BSA was fixed at 1.0×10^{-5} mol L^{-1}. From (a) to (g), the concentrations of CdSeS QDs were 0, 1.25×10^{-5}, 2.50×10^{-5}, 3.75×10^{-5}, 5.00×10^{-5} and 6.25×10^{-5} mol L^{-1}, successively.

Table 1
Stern–Volmer quenching constants of the QDs–BSA system at different temperatures.

T(K)	K_{sv} (L mol^{-1})	K_q (M^{-1} s^{-1})	R
286	1.35×10^4	1.35×10^{12}	0.997
291	1.23×10^4	1.23×10^{12}	0.998
296	1.11×10^4	1.11×10^{12}	0.995

concentration of quencher (CdSeS QDs), τ_0 is the lifetime and K_{sv} is the Stern–Volmer quenching constant. Since the lifetime τ_0 for the biomacromolecule is often taken as 10^{-8} s [24], the bimolecular quenching rate constants (K_q) could be easily obtained. Inset of Fig. 5 shows that the plots of (F_0/F) versus [Q] present a positive deviation (concave towards the y-axis) at all studied temperatures, indicating the presence of both static and dynamic quenching [25]. After linear fit at low concentrations (1.0×10^{-5}–6.0×10^{-5} M), quenching constants K_{sv} were calculated from the slope of the Stern–Volmer plots and the results were shown in Table 1. Evidently, K_{sv} is inversely correlated with temperature, indicating that the possible quenching mechanism in the fluorescence intensities of BSA is induced by complex formation rather than by dynamic collision [26]. Meanwhile, the bimolecular quenching constants K_q were calculated to be 1.35×10^{12} L mol^{-1} s^{-1} at 286 K, 1.23×10^{12} L mol^{-1} s^{-1} at 291 K and 1.11×10^{12} L mol^{-1} s^{-1} at 296 K, all significantly larger than the maximum scatter collision quenching constant of various quenchers with the biopolymer in (2.0×10^{10} L mol^{-1} s^{-1}) [27,28]. These results also prove that the quenching of the fluorescence intensity in nature is mainly from static quenching rather than dynamic quenching. So, a ground state complex is probably formed between BSA and CdSeS QDs that leads to this intrinsic fluorescence quenching. The similar results were also shown in the interaction study of MPA-capped CdTe [12] and CdS QDs [29] with BSA, which preliminarily proved that the nature of quenching of QDs on BSA is probably dependent on the functional group capped in the surface of QDs when the molecular volume size varies little, rather than the core material, though the binding forces were different. As revealed by the literature [30], the functional group of QDs is an important influencing factor in interactions between QDs and BSA.

3.2.2. Conformation investigation

In order to further study the structural change of BSA induced by CdSeS QDs, the UV–visible absorption spectra, synchronous fluorescence spectra and CD spectra of BSA with the addition of various concentrations of QDs were also measured.

UV–visible absorption is a simple method to investigate the structural change of the protein and the complex formation in a donor–acceptor system [31,32]. In the present study, we have measured UV–vis absorption spectra of BSA in the absence and presence of CdSeS QDs and the results are presented in Fig. 5. With the addition of CdSeS QDs, the absorption intensity of BSA increased gradually along with a slight blueshift from 278 nm to 276 nm, reconfirming that there is the ground state complex formation between BSA and CdSeS QDs because dynamic quenching does not change the absorption spectra while the formation of ground state complex, that is, static quenching often leads to a change in the absorption spectra [22]. Similar results were also observed in the study of L-cysteine capped CdSe/CdS QDs and thioglycolic acid capped CdTe QDs on BSA [13,33]. The blue shift of absorption peaks showed the peptide strands of BSA molecules extended more and the hydrophobicity was decreased [12–13,31]. According to the literature, the equilibrium for the formation of the complex between BSA and colloidal CdSeS QDs can be given described by Hildebrand group [34]:

$$\frac{1}{A_{obs}-A_0}=\frac{1}{A_c-A_0}+\frac{1}{K_{app}(A_c-A_0)[QDs]}. \quad (2)$$

where A_{obs} is the observed absorbance of the solution containing different concentrations of the colloidal CdSeS QDs at 280 nm, A_0 and A_c are the absorbances of BSA and the complex at 280 nm, respectively, and K_{app} is the apparent association constant. The values of $(A_{obs}-A_0)^{-1}$ were calculated and plotted against quencher concentration $[QDs]^{-1}$ according to Eq. 2 as shown in the inset of Fig. 5. After linear fit, the calculated value of K_{app} based on the slope and intercept of the plot is about 1.56×10^4 M^{-1} (R=0.9946), which is smaller than the apparent association constant between green MPA-capped CdTe QDs and BSA (1.72×10^5 M^{-1}) [35]. This result agrees well with the conclusion that larger sized QDs show stronger binding force upon interaction with BSA, as the alloyed CdSeS QDs (2.1 nm) are smaller than the green CdTe QDs (2.5 nm) [27, 35].

Synchronous fluorescence spectroscopy is a useful technique to separate the overlapped excitation peaks of aromatic amino acid residues of protein, which offers the information on the microenvironment changes of the residues by measuring the possible shift in wavelength emission maximum [33,35]. The synchronous fluorescence spectra of BSA contributing to tyrosine and tryptophan residues were recorded by a simultaneous scanning of the excitation and emission wavelengths in the 15- and 60-nm wavelength intervals and the data are presented in Fig. 6. In the absence of CdSeS QDs, the main peak of BSA at 287 nm arises from tyrosine residues (Fig. 6A, a), and the peak at 283 nm is attributed to tryptophan residues (Fig. 6B, a). In the presence of various concentrations of CdSeS QDs, the fluorescence quenching of BSA (Fig. 6, b–h) is consistent with the results of the fluorescence spectra (Fig. 4). The results show that energy transfer might occur from tyrosine and tryptophan residues to the CdSeS QDs. With the gradual addition of CdSeS QDs, there is no noticeable shift in position of emission wavelength corresponding to tyrosine residues (Fig. 6A) and a slight redshift from 283 to 285 nm for tryptophan residues (Fig. 6B). For aromatic tyrosine and tryptophan residues of BSA molecule, the fluorescence emission peak is sensitive to the polarity of its microenvironment. The

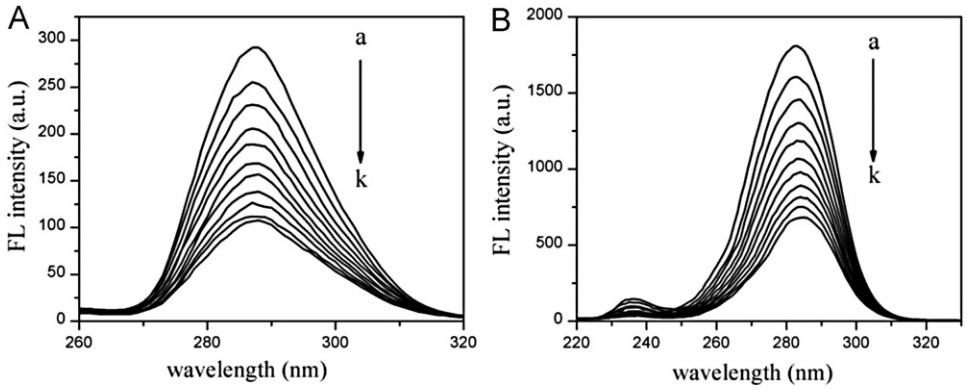

Fig. 6. Synchronous fluorescence spectra of BSA in the influence of various concentrations of CdSeS QDs: (A) $\Delta\lambda=15$ nm and (B) $\Delta\lambda=60$ nm. The concentration of BSA was fixed at 1.0×10^{-6} mol L^{-1}. From (a) to (k), the concentrations of CdSeS QDs were 0, 3.0×10^{-6}, 6.0×10^{-6}, 9.0×10^{-6}, 1.2×10^{-5}, 1.5×10^{-5}, 1.8×10^{-5}, 2.1×10^{-5}, 2.4×10^{-5}, 2.7×10^{-5} and 3.0×10^{-5} mol L^{-1}, successively.

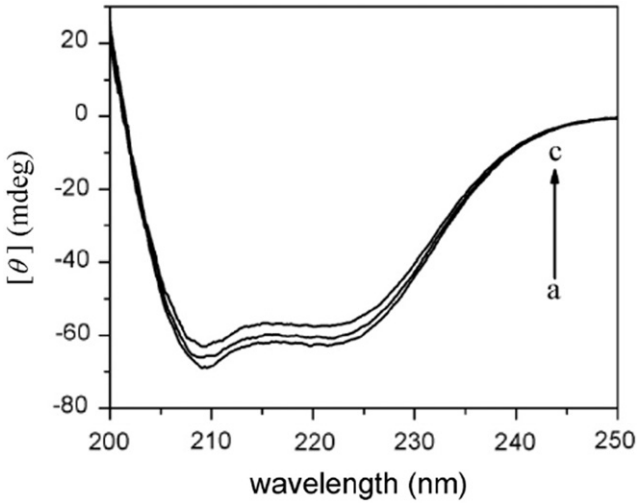

Fig. 7. CD spectra of BSA obtained in 0.1 M PBS solution (pH 7.4) at room temperature in the absence and presence of CdSeS QDs. The concentration of BSA was fixed at 5.0×10^{-6} mol L^{-1} (a). In the BSA–QDs system, the QDs concentration was 0.625 (b) and 1.250×10^{-6} mol L^{-1} (c).

redshift suggests that the fluorescing aromatic residues buried in nonpolar hydrophobic environment are moved to a hydrophilic environment; on the contrary, the blueshift signifies an enhancement of hydrophobicity [36]. The redshift observed in Fig. 6B shows that binding of CdSeS QDs probably induces the tertiary structural changes of the adsorbed BSA, and increased the polarity around the tryptophan residues. Similar observation was reported when mercaptoacetic acid capped CdTe QDs (3.0 nm) were adopted to bind with BSA [33]. However, a blueshift was obtained when starch capped CdS nanoparticles were used [37], implying that the functional group on the surface of QDs and the size of QDs played an important role in the interactions between QDs and BSA [30].

CD spectroscopy is a sensitive technique to study the conformation of proteins in aqueous solution [38–40], which can provide additional evidence for the possible conformational changes of BSA with the addition of CdSeS QDs and the results were presented in Fig. 7. The CD spectrum of BSA in the absence of CdSeS QDs exhibits two pronounced negative bands at about 208 and 222 nm, which is the characteristic feature of a high α-helical content of protein [41]. In the BSA–QDs system, the CD spectra of BSA showed similar shape with that of unbound BSA, indicating that the structure of BSA is also predominantly α-helical [42]. With the addition of QDs solution, the intensity of the negative bands at 208 and 222 nm decreased slightly compared to that of free BSA, implying that there is moderate perturbation of secondary and tertiary structures by the binding of QDs, which reconfirms that CdSeS QDs were bound to BSA to form a ground state complex. Based on mean residue ellipticity and the equation described by Seetharamappa group [43], the α-helical contents in the secondary structures of BSA were calculated to be 64.52% in unbound BSA and 58.79% in the BSA–QDs system (mol ratio 5:1.25), respectively. The decrease in α-helical content indicates that the CdSeS QDs bind with the amino acid residues of the main polypeptide chain of BSA and destroyed their hydrogen bonding networks [44]. So BSA molecules probably adopt a looser conformation in the presence of QDs which leads to the exposure of the hydrophobic cavities. And the conclusion is consistent with the result of synchronous fluorescence spectra experiment. Furthermore, the secondary structure contents are related close to the biological activity of BSA [35]. So a decrease in α-helical indicates the loss of the biological activity of BSA upon interaction with the as-prepared CdSeS QDs, implying the QDs' toxicity on protein.

4. Conclusion

In this work the synthesis of small sized alloyed CdSeS QDs in aqueous phase using microwave irradiation was shown. Also, the biological toxicity targeted to BSA was evaluated through multi-spectroscopic techniques. The experimental results indicated that the probable quenching mechanism of BSA fluorescence by alloyed CdSeS QDs was mainly static quenching process, that is, the formation of non-fluorescence ground-state complex and the nature of quenching of QDs on BSA is probably dependent on the surface functional groups. That is to say, the quenching mechanism of QDs on BSA has more to do with the surface materials rather than with the core materials when the size of QDs varies little, though their binding mode and binding strength are different. Additionally, the results of UV–vis absorption spectra, synchronous fluorescence spectra and CD spectra proved that the addition of QDs changed the conformation of BSA molecules, which induced toxic effects.

Acknowledgment

We acknowledge the financial support from the National High Technology Research and Development Program of China (863 program, No. 2007AA06Z418), the National Natural Science Foundation of China (Nos. 20577036, 20777058, 20977070), the Open Fund of Hubei Biomass-Resource Chemistry and Environmental Biotechnology Key Laboratory (HBRCEBL2011-2012005) and the Fundamental Research Funds for the Central Universities.

References

[1] M. Bruchez, M. Moronne, P. Gin, S. Weiss, A.P. Alivisatos, Science 281 (1998) 2013.
[2] W.C. Chan, S. Nie, Science 281 (1998) 2016.
[3] J. Zayed, S. Philippe, Int. J. Toxicol. 28 (2009) 259.
[4] S.J. Cho, D. Maysinger, M. Jain, B. Rer, S. Hackbarth, F.M. Winnik, Langmuir 23 (2007) 1974.
[5] A.O. Choi, S.J. Cho, J. Desbarats, J. Lovric, D. Maysinger, J. Nanobiotechnol. 5 (2007) 1.
[6] A. Zintchenko, A.S. Susha, M. Concia, J. Feldmann, E. Wagner, A.L. Rogach, M. Ogris, Mol. Ther. 17 (2009) 1849.
[7] E. Przybytkowski, M. Behrendt, D. Dubois, D. Maysinger, FEBS J. 276 (2009) 6204.
[8] R. Hardman, Environ. Health Perspect. 114 (2006) 165.
[9] K. Yamasaki, T. Maruyama, U. Kragh-Hansen, M. Otagiri, Biochim. Biophys. Acta 1295 (1996) 147.
[10] J. Liang, Y. Cheng, H. Han, J. Mol. Struct. 892 (2008) 116.
[11] S. Dilson, M.C. Celia, C.B. Jayme, L. Sonia, Toxicol. Lett. 147 (2004) 53.
[12] L. Zhao, R. Liu, X. Zhao, B. Yang, C. Gao, X. Hao, Y. Wu, Sci. Total Environ. 407 (2009) 5019.
[13] L. Ding, P.J. Zhou, S.Q. Li, G.Y. Shi, T. Zhong, M. Wu, J. Fluoresc. 21 (2010) 17.
[14] M. Ghali, J. Lumin. 130 (2010) 1254–1257.
[15] H.F. Qian, L. Li, J.C. Ren, Mater. Res. Bull. 40 (2005) 726.
[16] P.P. Hankare, V.M. Bhuse, K.M. Garadkar, A.D. Jadhav, Mater. Chem. Phys. 71 (2001) 53.
[17] G.A. Crosby, J.N. Demas, J. Phys. Chem. 75 (1971) 991.
[18] C. Wurth, M. Grabolle, J. Pauli, M. Spieles, U. Resch-Genger, Anal. Chem. 83 (2011) 3431.
[19] A. Wolcott, D. Gerion, M. Visconte, J. Sun, A. Schwartzberg, S. Chen, J.Z. Zhang, J. Phys. Chem. B 110 (2006) 5779.
[20] M. Idowu, E. Lamprecht, T. Nyokong, J. Photochem. Photobiol. A 198 (2008) 7.
[21] J. Xiao, Y. Bai, Y. Wang, J. Chen, X. Wei, Spetrochim. Acta A 76 (2010) 93.
[22] J.R. Lakowicz, Principles of Fluorescence Spectroscopy, 3rd ed., Springer, New York, 2006.
[23] O.R. Quayle, Chem. Rev. 53 (1953) 439.
[24] W.R. Ware, J. Phys. Chem. 66 (1962) 455.
[25] S.M.T. Sheikh, J. Seetharamappa, S. Ashoka, P.B. Kandagal, Dyes Pigments 73 (2007) 211.
[26] Q. Xiao, S. Huang, Z.D. Qi, B. Zhou, Z.K. He, Y. Liu, Biochim. Biophys. Acta 2008 (1784) 1020.
[27] J.B. Xiao, X.Q. Chen, X.Y. Jiang, M. Hilczer, M. Tachiya, J. Fluoresc. 18 (2008) 671.
[28] H. Cao, D.H. Wu, H.X. Wang, M. Xu, Spectrochim. Acta A 73 (2009) 972.
[29] D. Huang, F. Geng, Y. Liu, X. Wang, J. Jiao, L. Yu, Colloid Surf. A: Physicochem. Eng. Aspects 392 (2011) 191.
[30] J.J. Ma, J.G. Liang, H.Y. Han, Spectrosc. Spectral Anal. 30 (2010) 1039.
[31] Y.J. Hu, Y. Liu, J.B. Wang, X.H. Xiao, S.S. Qu, J. Pharm. Biomed. Anal. 36 (2004) 915.
[32] S. Bi, D. Song, Y. Tian, X. Zhau, Z. Liu, H. Zhang, Spectrochim. Acta A 61 (2005) 629.
[33] J. Fan, J. Zhou, T. Sun, S. Lv, J. Tang, J. Lv, Chin. J. Chem. 28 (2010) 2353.
[34] H.A. Benesi, J.H. Hildebrand, J. Am. Chem. Soc. 71 (1949) 2703.
[35] Q. Wang, P. Liu, X. Zhou, X. Zhang, T. Fang, P. Liu, X. Min, X. Li, J. Photochem. Photobiol. A 230 (2012) 23.
[36] C.W. Liu, A.L. Bo, G.J. Cheng, X.Q. Lin, S.J. Dong, Biochim. Biophys. Acta 1385 (1998) 53.
[37] M.A. Jhonsi, A. Kathiravan, R. Renganathan, Colloid Surf. B 72 (2009) 167.
[38] X.C. Shen, X.Y. Liu, H. Liang, X. Lu, Acta Chim. Sin. 64 (2006) 469.
[39] S. Venkateshrao, P.T. Manoharan, Spectrochim. Acta A 60 (2004) 2523.
[40] N. Sreerama, R.W. Woody, Anal. Biochem. 287 (2000) 252.
[41] J. Liu, J. Tian, W. He, J. Xie, Z. Hu, X. Chen, J. Pharm. Biomed. Anal. 35 (2004) 671.
[42] Y. Hu, Y. Liu, X. Shen, X. Fang, S. Qu, J. Mol. Struct. 738 (2005) 143.
[43] S. Ashoka, J. Seetharamappa, P.B. Kandagal, S.M.T. Shaikh, J. Lumin. 121 (2006) 179.
[44] F.L. Cui, J. Fan, J.P. Li, Z.D. Hu, Bioorg. Med. Chem. 12 (2004) 151.